Inorganic Chemistry

Article

pubs.acs.org/IC

Syntheses and Excitation Transfer Studies of Near-Orthogonal Free-Base Porphyrin–Ruthenium Phthalocyanine Dyads and Pentad

Rachel Jacobs,[†] Kati Stranius,[‡] Eranda Maligaspe,[†] Helge Lemmetyinen,[‡] Nikolai V. Tkachenko,*[,‡] Melvin E. Zandler,[†] and Francis D'Souza*[,†,§]

[†]Department of Chemistry, Wichita State University, 1845 Fairmount, Wichita, Kansas 67260-0051, United States

[‡]Department of Chemistry and Bioengineering, Tampere University of Technology, P.O. Box 541, 33101 Tampere, Finland

[§]Department of Chemistry, University of North Texas, 1155 Union Circle, 305070, Denton, Texas 76203-5017, United States

Supporting Information

ABSTRACT: A new series of molecular dyads and pentad featuring free-base porphyrin and ruthenium phthalocyanine have been synthesized and characterized. The synthetic strategy involved reacting free-base porphyrin functionalized with one or four entities of phenylimidazole at the meso position of the porphyrin ring with ruthenium carbonyl phthalocyanine followed by chromatographic separation and purification of the products. Excitation transfer in these donor–acceptor polyads (dyad and pentad) is investigated in nonpolar toluene and polar benzonitrile solvents using both steady-state and time-resolved emission techniques. Electrochemical and computational studies suggested that the photoinduced electron transfer is a thermodynamically unfavorable process in nonpolar media but may take place in a polar environment. Selective excitation of the donor, free-base porphyrin entity, resulted in efficient excitation transfer to the acceptor, ruthenium phthalocyanine, and the position of imidazole linkage on the free-base porphyrin could be used to tune the rates of excitation transfer. The singlet excited Ru phthalocyanine thus formed instantly relaxed to the triplet state via intersystem crossing prior to returning to the ground state. Kinetics of energy transfer (k_{ENT}) was monitored by performing transient absorption and emission measurements using pump–probe and up-conversion techniques in toluene, respectively, and modeled using a Förster-type energy transfer mechanism. Such studies revealed the experimental k_{ENT} values on the order of 10^{10}–10^{11} s^{-1}, which readily agreed with the theoretically estimated values. Interestingly, in polar benzonitrile solvent, additional charge transfer interactions in the case of dyads but not in the case of pentad, presumably due to the geometry/orientation consideration, were observed.

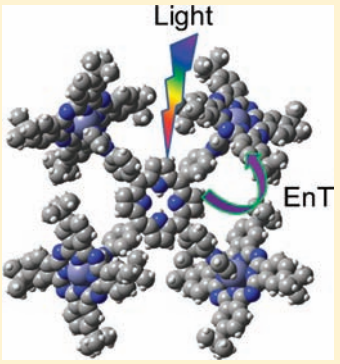

INTRODUCTION

Solar energy technologies are the most promising solution for sustainable energy production. Sunlight constitutes the primary energy source for almost all of the interdependent biological events in nature, thus making life possible.[1,2] For developing efficient and affordable light energy harvesting systems, molecular systems capable of collecting, translating, and accumulating sunlight are desirable toward clean energy production. However, design of such multifaceted devices requires building multicomponent arrays of units by a modular approach such that they perform key functions of photosynthesis, viz., energy capture and funneling, and electron transfer, ultimately creating the energetic oxidizing and reducing equivalents of sufficient lifetimes (milliseconds to seconds).[3−11]

This approach is for not only useful building artificial photosynthetic devices but also photovoltaics and optoelectronic applications.[12]

In natural photosynthesis, energy capture and funneling (converting the energy of an absorbed photon into an electron excitation) has efficiently been done by chlorophylls and carotenoids that are supramolecularly organized for unidirectional excitation transfer toward a reaction center.[1,2] Researchers have been attempting to mimic this process with the help of molecular donor–acceptor systems combining two or more chromophores.[3−11] These chromophores are covalently linked,[13−16] form part of a polymer system,[17] associated with a dendrimeric structure,[18] or self-assembled systems by intermolecular forces.[19] Due to their structural similarity to the natural light harvesting chlorophyll material and the established synthetic methodologies and their outstanding electronic properties, in a majority of these studies porphyrins[20] and phthalocyanines[21] have been used as common chromophores. Evidently, several dyads featuring these two chromophores have been reported.[22]

Recently, we reported on free-base porphyrin–Zn (or Mg) phthalocyanine (or naphthalocyanine) dyads via metal–ligand axial coordination and reported ultrafast singlet–singlet excitation transfer.[23] Although phenylimidazole-functionalized porphyrin was used to achieve a higher stability of the complexes instead of more the traditional pyridine-functionalized porphyrin, it was not possible to isolate the complexes due

Received: November 29, 2011
Published: March 5, 2012

   dx.doi.org/10.1021/ic202574q | Inorg. Chem. 2012, 51, 3656–3665

Chart 1. Structure of the Dyads and Pentad Developed in the Present Study To Probe Excitation Energy Transfer

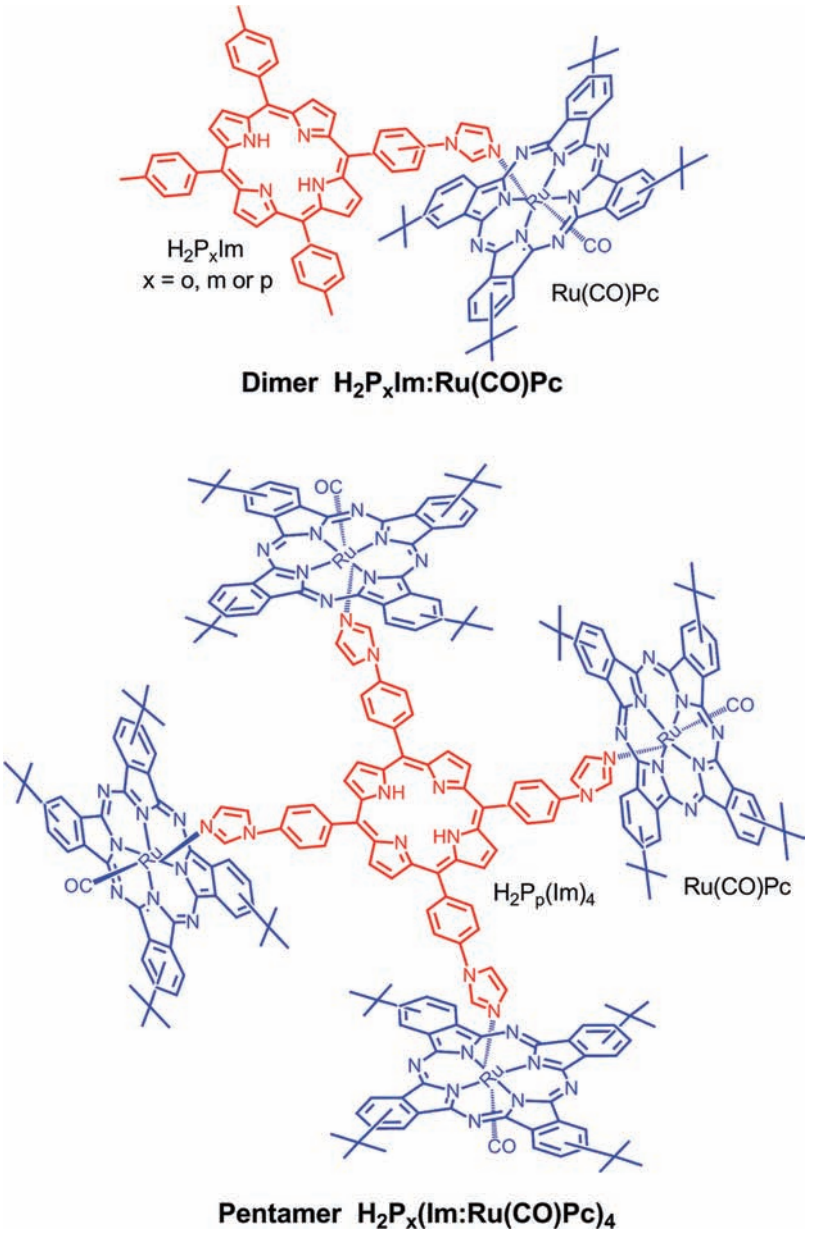

to the labile nature of the metal–ligand coordinate bond. Hence, the synthetic protocol could not be extended to create a higher version of the polyads (triads, tetrads, pentads, etc.) as biomimetic multicomponent energy funneling antenna models. To overcome this issue, in the present study we employed ruthenium carbonyl phthalocyanine, Ru(CO)*Pc*, instead of their Zn or Mg phthalocyanines and synthesized dyads using 2-, 3-, or 4-imidozylphenyl-substituted free-base porphyrins. Further, this strategy has been extended to form a pentad using a porphyrin functionalized with four entities of 4-imidozylphenyl substituents at the porphyrin periphery (Chart 1). Different substitution resulted in dyads of different orientations. Photochemical studies using both steady-state and time-resolved emission techniques have been performed to probe the efficiency and kinetics of excitation transfer in the newly formed dyads and pentad.

RESULTS AND DISCUSSION

Synthesis of the Dyads and Pentad. Porphyrins bearing an imidazole group at one of its meso phenyl positions have been synthesized by reaction of stoichiometric amounts of pyrrole, tolualdehyde, and 4-imidazolylbenzaldehyde using the standard procedure.[20] The imidazole entity on the phenyl group was functionalized at the ortho, meta, or para positions to visualize the relative orientation of the donor–acceptor entities on their photochemical properties. For formation of pentad, all of the meso positions have been substituted with 4′-imidazolyl benzene groups. The employed phthalocyanine had four *tert*-butyl substituents at the periphery to improve its solubility and reduce aggregation without significantly perturbing the electronic structure in organic solvents. Ru(CO)*Pc* was synthesized in good yields by reaction of free-base phthalocyanine with trisruthenium dodecacarbonyl in phenol following the literature procedure.[24] The choice of the CO group on Ru(CO)*Pc* provided stronger ligation due to the π-acceptor

dx.doi.org/10.1021/ic202574q | *Inorg. Chem.* 2012, 51, 3656–3665

carbonyl ligand at one of the two axial Ru(II) coordination sites. Syntheses of the dyads and pentad involved reacting stoichiometric amounts of imidazole-functionalized porphyrin with Ru(CO)*Pc* followed by chromatographic separation. This approach has earlier been used to form molecular architectures using various pyridine-derivatized molecular components.[25] The present method differs from the earlier method where imidazole–ruthenium binding instead of pyridine–ruthenium was successfully used.[24] As shown here, due to the better ligating behavior of imidazole, the synthetic methodology has been facile, resulting in higher yields of products. The newly synthesized compounds were purified over a silica gel column prior to performing spectral measurements and characterized by mass spectrometry, NMR spectroscopy, and other methods. Additionally, thin-layer chromatography (TLC) on all of the newly synthesized compounds was performed to ensure the absence of impurities.

Optical Absorption Spectral Studies. Figure 1 shows the optical absorption spectra of the newly synthesized compounds

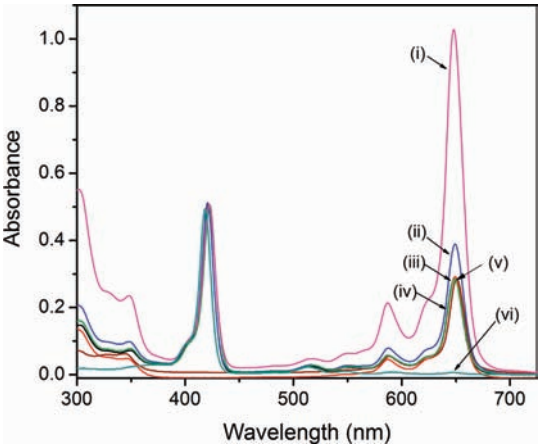

Figure 1. Normalized to the porphyrin Soret band absorption spectra of (i) H_2P_p(Im:Ru(CO)*Pc*)$_4$ pentad, (ii) H_2P_mIm:Ru(CO)*Pc* dyad, (iii) H_2P_pIm:Ru(CO)*Pc* dyad, (iv) H_2P_oIm:Ru(CO)*Pc* dyad, (iv) PhIm:Ru(CO)*Pc*, (v) Ru(CO)*Pc*, and (vi) H_2TPP in toluene.

along with the control compounds normalized to the porphyrin Soret band. The free-base porphyrin, H_2TPP (or H_2P_xIm derivatives in Chart 1), has a Soret band at 418 nm and four less intense visible bands. Both Ru(CO)*Pc* and PhIm:Ru(CO)*Pc*, the control compound synthesized by reacting phenyl imidazole and Ru(CO)*Pc* (the colon symbol represents the metal–ligand axial bond), revealed a strong absorption band at 650 nm accompanied by weaker absorption bands at 587 and 346 nm. For the dyads, the spectral features were similar to the 1:1 mixture of H_2TPP and PhIm:Ru(CO)*Pc* with less than a 1 nm red shift of the porphyrin Soret and less than 2 nm blue shift of the phthalocyanine absorption band positions. For the pentad, the phthalocyanine peak intensity was nearly four times that of the dyads with less than a 2 nm change in spectral peak positions, providing proof for the structural integrity of the pentad. It is important to note that the 516 nm peak of H_2P had no significant spectral overlap with Ru(CO)*Pc* absorption bands, suggesting this wavelength is suitable for selective excitation of the porphyrin in the dyads and pentad.

Steady-state fluorescence spectra of the compounds are shown in Figure 2. Pristine H_2TPP (or H_2P_xIm derivatives in

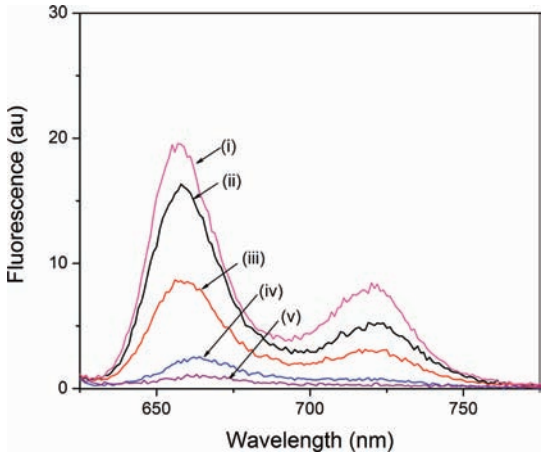

Figure 2. Fluorescence emission spectra of (i) H_2P_oIm:Ru(CO)*Pc* dyad, (ii) H_2P_pIm:Ru(CO)*Pc* dyad, (iii) H_2P_mIm:Ru(CO)*Pc* dyad, (iv) H_2P_p(Im:Ru(CO)*Pc*)$_4$ pentad, and (v) Ru(CO)*Pc* in toluene. λ_{ex} = 518 nm. Concentrations were held at 10 μM.

Chart 1) revealed emission bands at 650 and 720 nm. For all of the dyads and pentad, the porphyrin emission bands were found to be quenched over 95% of their initial intensity, more so for the pentad (97%), accompanied by red shifts of ~6 nm for the dyads and 12 nm for the pentad (see Supporting Information Figure S1 for comparative emission spectra with respect to H_2TPP emission). Interestingly, under the experimental conditions used, Ru(CO)*Pc* revealed a very weak emission at 670 nm. Direct excitation of Ru(CO)*Pc* at any of its absorption peak maxima also revealed weak emission at 670 nm, indicating very low emission quantum yields. This property has earlier been attributed to the gradually quenched emission of the phthalocyanine singlet excited state which undergoes rapid intersystem crossing populating the triplet state due to the presence of a heavy atom in the phthalocyanine cavity.[24a] The small red shift in H_2P emission could be ascribed to axial coordination and/or overlap of Ru(CO)*Pc* emission as a result of energy transfer.

To unravel the quenching mechanism of the porphyrin fluorescence as to energy or electron transfer, further electrochemical and computational studies were performed, as summarized below.

Electrochemical and Computational Studies. Figure 3 shows the cyclic voltammograms of Ru(CO)*Pc* and

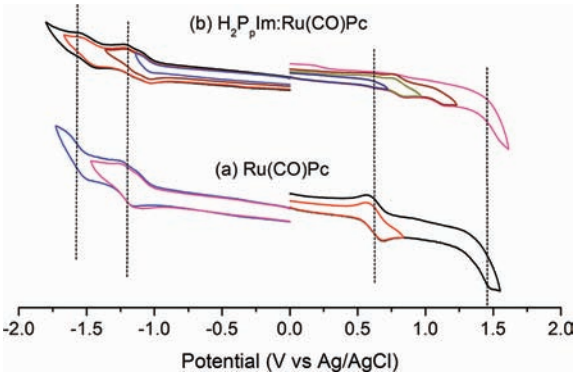

Figure 3. Cyclic voltammograms of (a) Ru(CO)*Pc* and (b) H_2P_pIm:Ru(CO)*Pc* dyad (~0.5 mM) in *o*-dichlorobenzene containing 0.1 M (TBA)ClO_4. Scan rate = 100 mV/s.

dx.doi.org/10.1021/ic202574q | *Inorg. Chem.* 2012, 51, 3656–3665

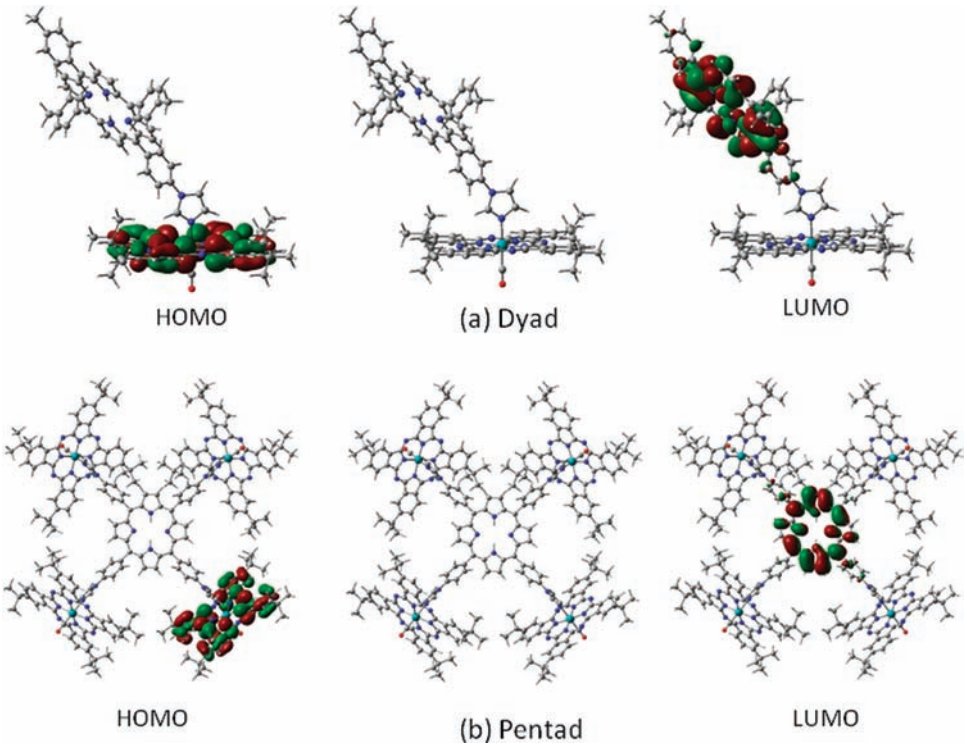

Figure 4. B3LYP/3-21G(*)-optimized structures of the (a) H_2P_pIm:Ru(CO)*Pc* dyad and (b) H_2P_p(Im:Ru(CO)*Pc*)$_4$ pentad. HOMO and LUMO of the respective compounds are shown in the left and right side of each optimized structure.

H_2P_pIm:Ru(CO)*Pc* in *o*-dichlorobenzene containing 0.1 M (TBA)ClO_4. For electrochemical measurements we used *o*-dichlorobenzene instead of toluene due to insolubility of the supporting electrolyte in the latter solvent. The precursor, Ru(CO)*Pc* revealed the first reversible oxidation at 0.61 V and a second one at 1.43 V vs Ag/AgCl. The first two reversible reductions of Ru(CO)*Pc* were located at −1.20 and −1.57 V vs Ag/AgCl. In agreement with earlier reports,[24] these electrode processes were all macrocycle based and had no metal center involved. The first reversible oxidation and first two reversible reductions of H_2P_oIm were located at 0.55 and −1.67 and −2.02 V vs Fc/Fc$^+$ in 0.1 (TBA)ClO_4, respectively.[23a] For H_2P_mIm and H_2P_pIm, the first reduction was shifted in the negative direction by 50−60 mV while the first oxidation was anodically shifted by 40 mV.[23a] The dyad, H_2P_pIm:Ru(CO)*Pc*, revealed four oxidations located at 0.62, 0.80, 1.09, and 1.45 V vs Ag/AgCl and four reductions located at −1.12, −1.20, −1.49, and −1.58 V vs Ag/AgCl. By comparing the redox potential values with those of Ru(CO)*Pc* and H_2TPP (or H_2P_xIm derivatives), the first and fourth oxidation and second and fourth reductions of the dyad were ascribed to the Ru(CO)*Pc* entity while the second and third oxidation and the first and third reduction processes were ascribed to the porphyrin entity. Consequently, the lowest energy required for the charge transfer reaction to occur is 1.74 eV, in which case electron transfer would take place from Ru(CO)*Pc* donor to H_2P_xIm acceptor. Very similar redox chemistry was observed for the other two dyads, while for the pentad the four equivalents of Ru(CO)*Pc* overpowered the currents of the redox waves in which case the redox processes of H_2P appeared as shoulder waves at almost the same potential values.

Figure 4 shows the structures of the H_2P_pIm:Ru(CO)*Pc* dyad and the H_2P_p(Im:Ru(CO)*Pc*)$_4$ pentad, energy optimized on a Born−Oppenheimer potential energy surface using the B3LYP/3-21G(*) method.[26,27] Similar structures were obtained for the other two dyads. In agreement with the results of earlier reported ZnPc- and MgPc-based dyads, the two macrocyclic porphyrin and phthalocyanine rings were found to be in a skipped coplanar arrangement with an angle less than a right angle between the two planes. The center-to-center distance between the two macrocycles ranged between 8 to 12 Å, while the edge-to-edge distances were between 5.7 and 8.8 Å, depending upon the position of substitution of the imidazole ring on the porphyrin macrocycle. Generally, the distances varied as ortho < meta < para imidazole-substituted porphyrins.

In the case of the H_2P_p(Im:Ru(CO)*Pc*)$_4$ pentad, the peripheral imidazole-coordinated Ru(CO)*Pc* entities were positioned about 50° to the plane of the porphyrin ring. In addition, two of the four Ru(CO)*Pc* macrocycles positioned at opposite side of the porphyrin macrocycle had the same orientation while the other two Ru(CO)*Pc* macrocycles had an opposite orientation (roughly a C_2 rotation axis). As a result, the four Ru centers created a dihedral angle of about 25°. The Ru−Ru distance from the neighboring macrocycles were in the range of 18.6−19.9 Å, while the distance between Ru and the center of free-base porphyrin was ∼13.2 Å. The Ru−Ru distance between the oppositely positioned Ru(CO)*Pc* rings were 23.6 and 25.9 Å.

The frontier orbitals, HOMO and LUMO, were also evaluated for both dyads and the pentad, and the representative orbitals are shown in Figure 4. The HOMO for all of the studied polyads was fully localized on the Ru(CO)*Pc*, while the LUMO was located on the free-base porphyrin macrocycle. In agreement with the electrochemical results, these results point out that the lowest energy charge transfer state is $H_2P_pIm^{-\bullet}$:Ru(CO)*Pc*$^+$. The gas-phase HOMO−LUMO gap for the dyads was ∼2.06 eV, which was slightly larger than that of the pentad, 1.90 eV.

dx.doi.org/10.1021/ic202574q | *Inorg. Chem.* 2012, 51, 3656−3665

Using the electrochemical, computational, and emission data, the free energies of charge separation (ΔG_{CS}) were calculated using eq 1 by Weller's approach[28]

$$-\Delta G_{CS} = \Delta E_{0-0} - e(E_{ox} - E_{red}) + \Delta G_S \quad (1)$$

where ΔE_{0-0} is the energy of the lowest excited state of the fluorophore (1.90 eV for H_2P and 1.85 eV for Ru(CO)*Pc*), E_{ox} and E_{red} represent, respectively, the first oxidation of the donor and first reduction of the acceptor, $\Delta G_S = -e^2/(4\pi\varepsilon_0\varepsilon_R R_{Ct\text{-}Ct})$, and ε_0 and ε_R refer to the vacuum permittivity and dielectric constant of the solvent. The lowest energy charge-separated state, $H_2P_pIm^{-\bullet}$:Ru(CO)$Pc^{+\bullet}$, is only 0.13 eV lower than the lowest singlet excited state Ru(CO)Pc^{S1} if the Coulombic term, ΔG_S, is neglected. Accounting for the Coulombic interaction makes photoinduced electron transfer an endothermic reaction in nonpolar and moderately polar solvents but slightly exothermic in polar media.

Excited Energy Transfer: Theoretical and Experimental Considerations. Since photoinduced electron transfer is not a likely mechanism based on energetic considerations, photoinduced energy transfer as a quenching mechanism was considered. Such an energy transfer between excited donor to an acceptor could be explained via either Dexter's exchange mechanism or Förster's dipole−dipole mechanism.[29] The former mechanism is based on double-electron exchange involving one electron from the LUMO of the excited donor to the empty LUMO of the acceptor with a simultaneous transfer of another electron from the HOMO of the acceptor to the half-filled HOMO of the donor.[29c] The rate constant is given by eq 2

$$k_D = 4\pi^2 H^2 J_D/h \quad (2)$$

where h is Plank's constant, H is the electronic exchange parameter, and J_D is the Dexter spectral overlap integral.[29c] The frontier orbitals from the B3LYP studies and the large separation between the donor and the acceptor entities (Figure 4) in conjunction with the spectroscopic studies reveal that such electronic interactions are almost nonexistent. Therefore, Förster's-type energy transfer mechanism is considered.

According to the Förster mechanism,[29b] the rate of excitation transfer, $k_{Förster}$, is given by eq 3

$$k_{Förster} = [8.8 \times 10^{-25}\kappa^2\Phi_D J_{Förster}]/[\eta^4\tau_D R^6] \quad (3)$$

where η is the solvent refractive index, Φ_D and τ_D are the fluorescence quantum yield (= 0.12) and fluorescence lifetime of the isolated donor (free-base porphyrin), $J_{Förster}$ is Forster's overlap integral representing the emission of the donor and absorption of the acceptor Ru(CO)*Pc*, and R is the donor−acceptor center-to-center distance. The τ_D values measured using the strobe technique were found to be 11.50, 9.95, and 9.45 ns, respectively, for the *o*-, *m*-, and *p*-imidazole-derivatived free-base porphyrins. In eq 3, κ^2 is the orientation factor as described in eq 4, often playing a key role in determining the efficiency of excitation energy transfer

$$\kappa^2 = [\cos\nu - 3\cos\alpha\cos\beta]^2 \quad (4)$$

where α and β are the angles made by the transition dipoles of the donor and acceptor entities with the line joining the centers of the transitions and ν is the angle between the two transition dipoles. The transition dipoles of tetrapyrroles is known to lie along a line joining two opposing pyrrole nitrogens.[30] The values of κ^2 evaluated based on computed optimum geometries of compounds are given in Table 1. It worth mentioning here that although the donor−acceptor are linked, there is enough flexibility in the dyads to deviate significantly from the low-energy-optimized structure. Under the condition of random dipole orientations one could assign a value of 2/3 for κ^2. Therefore, one can expect the actual values of κ^2 to be between the calculated ones and 2/3. The κ^2 value estimated for the meta derivative is close to this value. The κ^2 value estimated for the ortho derivative is much larger than 2/3 and is expected to be overestimated, whereas for the para derivative it is much lower than 2/3 and is expected to be underestimated.

Table 1. Förster Distance and Estimated ($k_{Förster}$) and Experimentally Determined (k_{ENT}) Rates of Energy Transfer for the Dyads and Pentad Formed by Coordination of Imidazole Appended Free-Base Porphyrin to Ru(CO) Phthalocyanine in Toluene

polyads[a]	κ^2	R_o (Å)	$k_{Förster}$ (s^{-1})[b]	k_{ENT} (s^{-1})[c]
H_2P_oIm:Ru(CO)*Pc*	3.25	26.20	5.18×10^{11}	1.25×10^{11}
H_2P_mIm:Ru(CO)*Pc*	0.82	26.19	1.24×10^{11}	7.14×10^{10}
H_2P_pIm:Ru(CO)*Pc*	0.12	26.18	1.56×10^{10}	3.22×10^{10}
H_2P_p(Im:Ru(CO)*Pc*)$_4$	0.14	26.43	1.82×10^{10}	3.71×10^{10}

[a]See Chart 1 for structures of different donor and acceptor entities. [b]Estimated according to eqs 3−5. Error = ±10%. [c]Determined from the pump−probe technique.

The spectral overlap integral, $J_{Förster}$, representing the emission of the donor and absorption of the acceptor is given by eq 5

$$J_{Förster} = F_D(\lambda)\varepsilon_A(\lambda)\lambda^4\, d\lambda \quad (5)$$

where $F_D(\lambda)$ is the fluorescence intensity of the donor with total intensity normalized to unity and $\varepsilon_A(\lambda)$ is the molar extinction coefficient of the acceptor expressed in units of M^{-1} cm^{-1} and λ in nanometers. Figure 5 shows the spectral overlap of the H_2PIm emission (donor) and Ru(CO)*Pc* absorption (acceptor) for the dyads. The $J_{Förster}$ values calculated based on eq 5 were in the range of 2.6−3.98 × 10^{-14} M^{-1} cm^3 for the investigated compounds. However, care must be exercised while using such results since the currently used donor and acceptor entities are known to have degenerate dipole

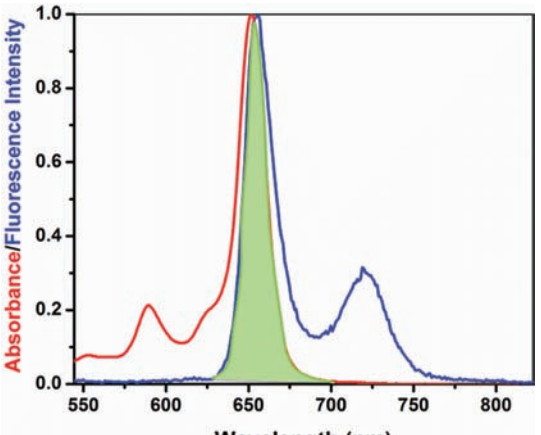

Figure 5. Spectral overlap (shaded area) for H_2PIm emission (donor) and Ru(CO)*Pc* absorption (acceptor) in toluene.

dx.doi.org/10.1021/ic202574q | *Inorg. Chem.* 2012, 51, 3656−3665

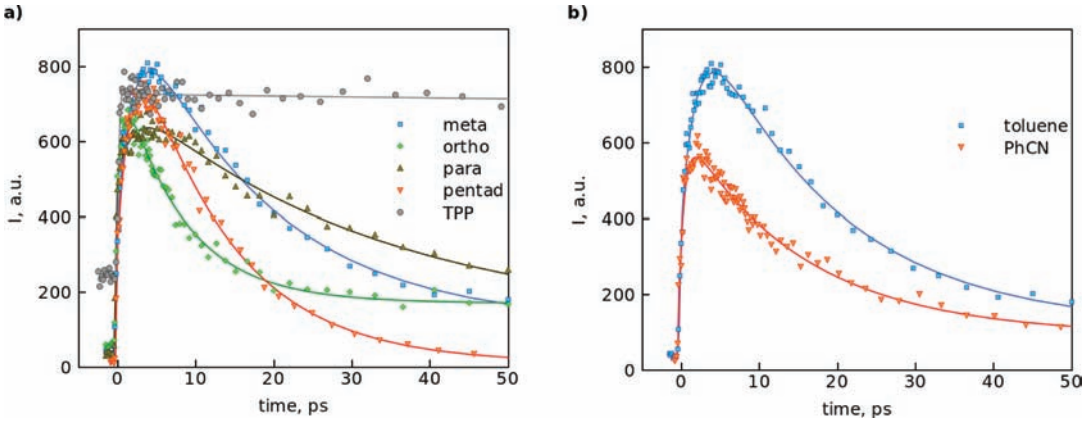

Figure 6. Emission decay curves for all compounds in toluene (a) and for H_2P_mIm:Ru(CO)*Pc* in toluene and PhCN (b).

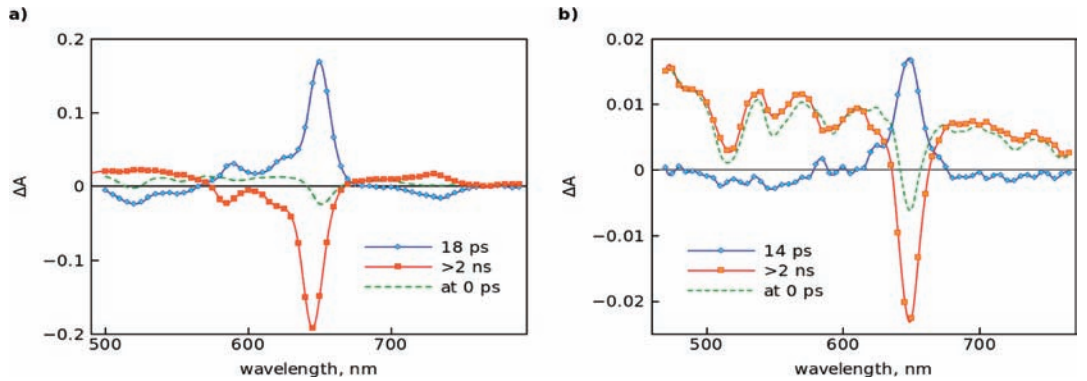

Figure 7. Transient absorption component and time-resolved (at zero delay) spectra (pump probe) of H_2P_mIm:Ru(CO)*Pc* in (a) toluene and (b) benzonitrile.

moments,[30] creating additional complications in estimating orientation-dependent rates, although such calculations serve as a very good tool to predict the experimental rate parameters (vide infra).

Equation 3 can be further simplified in terms of Förster distance, R_o, where one-half the donor molecules decay by energy transfer and one-half decay by the usual radiative and nonradiative mechanisms.[29a]

$$k_{\text{Förster}} = 1/\tau_D(R_o/R)^6 \quad (6)$$

The R_o and $k_{\text{Förster}}$ values estimated using the parameters described in eqs 2–6 were found to be about 26 Å and 10^{10}–10^{11} s^{-1}, predicting ultrafast energy transfer (Table 1). As explained in subsequent paragraphs, the rate of energy transfer measured using pump–probe and up-conversion techniques agrees well with predictions.

Up-Conversion and Pump–Probe Spectral Studies. Up-conversion measurements were carried out in a 1 mm rotating cuvette in both toluene and benzonitrile (PhCN) solvents. The excitation wavelength was set to 420 nm, while fluorescence decay was monitored at 720 nm, corresponding to porphyrin absorption and emission, respectively. Decays were measured in the time range of 200 ps, and the typical time resolution of the instrument was ~0.2 ps. Decay curves for the samples in toluene are shown in Figure 6a. The decay time constants are approximately the same in both solvents as presented by the example of the H_2P_mIm:Ru(CO)*Pc* dyad in Figure 6b (emission decays for all dyads and pentad in benzonitrile can be found in Supporting Information Figure S2). This suggests energy transfer as the main porphyrin fluorescence quenching mechanism.

The pump–probe measurements were also carried out in a 1 mm rotating cuvette. The excitation wavelength was 420 nm, and measurements were carried out in the wavelength range of 520–790 nm. The time resolution of the instrument was ~0.2 ps. Excitation was reduced to 20% of the maximum to ensure that no more than one chromophore in the dyads is excited at a time.

The results of the biexponential fit of pump–probe measurements of the H_2P_mIm:Ru(CO)*Pc* dyad in toluene are presented in Figure 7a. The time-resolved transient absorption spectrum right after excitation (at 0 ps) is essentially the spectrum of the porphyrin singlet excited state with characteristic holes at 515, 550, and 585 nm due to the Q-bands bleaching. This is expected since porphyrin absorption is much higher than that of phthalocyanine at the excitation wavelength, 420 nm. On the contrary, the spectrum of the longest lived component (>2 ns) is characteristic of the phthalocyanine excited state with clear bleaching of the phthalocyanine Q-bands at 585 and 645 nm and no signs of the porphyrin intermediates. Therefore, the component with a time constant of ~18 ps had straightforward interpretation, that is, quenching of the porphyrin singlet excited state by energy transfer to Ru(CO)*Pc*, the process in which the singlet excited state of porphyrin disappears and Ru(CO)*Pc* becomes involved into the excitation relaxation (bleaching of the Ru(CO)*Pc* Q-band). This is also in agreement with fluorescence decay measurements showing relaxation of the porphyrin singlet excited state with essentially the same time constant. However, the band at

dx.doi.org/10.1021/ic202574q | *Inorg. Chem.* 2012, 51, 3656–3665

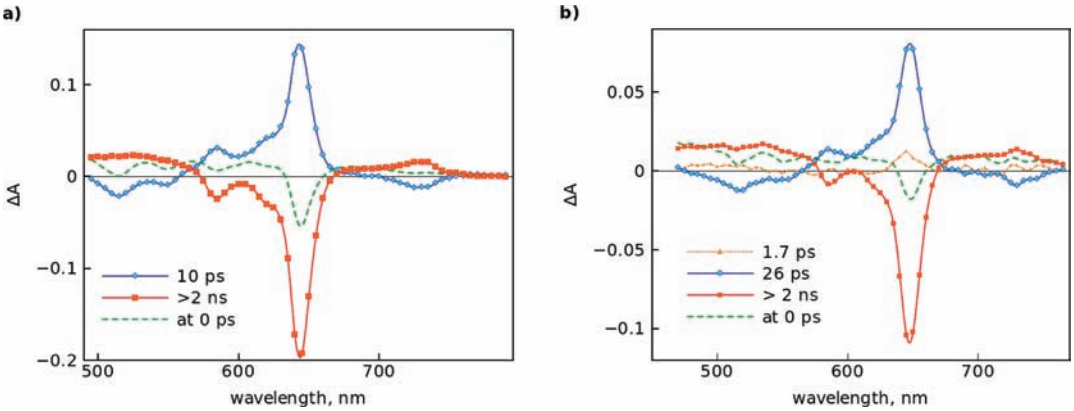

Figure 8. Transient absorption component and time-resolved (at zero delay) spectra (pump probe) of H_2P_p(Im:Ru(CO)*Pc*)$_4$ pentad in toluene (a) and benzonitrile (b).

720−730 nm is a characteristic feature of the Ru(CO)*Pc* triplet state, and it is formed with virtually the same time constant as the porphyrin singlet state decays. As stated earlier, although the energy transfer should take place between singlet states of H_2P_mIm and Ru(CO)*Pc*, $^*H_2P_mIm^{1S}$:Ru(CO)*Pc* → H_2P_mIm:*Ru(CO)Pc^{1S}, the intersystem crossing is rather fast for Ru(CO)*Pc*, in the range of 3−5 ps, i.e., faster than the energy transfer; thus, the singlet excited state of Ru(CO)*Pc* is not observed as it is converted almost instantly to the triplet state. This observation is fully in agreement with the steady-state fluorescence observations.

The results of the biexponential fit of pump−probe measurements of the H_2P_mIm:Ru(CO)*Pc* dyad in benzonitrile are presented in Figure 7b. Right after excitation (at 0 ps) the transient absorption spectrum revealed a clear feature of the H_2P_mIm singlet excited state, as can be expected, although some bleaching of the Ru(CO)*Pc* Q-band was seen at 650 nm. The following process with a time constant of 14 ps resulted in gradual enhancement of the Ru(CO)*Pc* Q-band bleaching and formation of the transient state with a differential spectrum presented by the longest lived component. The spectrum had clear features of ground state bleaching of both chromophores, H_2P_mIm and Ru(CO)*Pc*, indicating that H_2P_mIm does not return to the ground state on completion of the 14 ps process, which is in sharp contrast to the excitation relaxation in toluene. There is another clear difference between the long-lived states in toluene and benzonitrile in the red part of the spectrum, 670−780 nm. In toluene a relatively narrow band is seen around 720−730 nm, whereas in benzonitrile there was a strong broad absorption in the whole range 690−780 nm, which is indicative for Ru(CO)*Pc* cation radical.[24] At the same time, the 14 ps component indicates an increase in transient absorption around 570 nm, which is typical for a porphyrin transition from the singlet excited state to an anion radical.[11e] As suggested by the free-energy calculations, the electron transfer from *Ru(CO)Pc^1 to H_2P_mIm is possible in polar benzonitrile and may compete with the intersystem crossing process.

The other two dyads, H_2P_pIm:Ru(CO)*Pc* and H_2P_oIm:Ru(CO)*Pc*, revealed spectral features similar to the H_2P_mIm:Ru(CO)*Pc* dyad (see Supporting Information Figures S3 and S4 for spectral details). For the H_2P_pIm:Ru(CO)*Pc* dyad, a biexponential fit was sufficient for toluene, but for benzonitrile data, a three-exponential fit was needed. The emission decay measurements at 720 nm suggested that $^*H_2P_pIm^1$ decayed with a time constant of 30 ps in toluene and 28 ps in benzonitrile, respectively. For the H_2P_oIm:Ru(CO)*Pc* dyad, a two-exponential fit was sufficient for both solvents. The time constants for the reaction were 6 and 9 ps in toluene and benzonitrile, respectively.

Transient absorption spectra of the H_2P_p(Im:Ru(CO)*Pc*)$_4$ pentad in toluene and PhCN are presented in Figure 8. A biexponential fit was sufficient for toluene data, but for benzonitrile data three-exponential fit gave the best sigma value. The time constants of the reaction in toluene were 10 and 12 ps from transient absorption and emission decay fits, respectively. The results in PhCN differed from those of the H_2P_pIm:Ru(CO)*Pc* dyad in that the long-lived state (longer than a few hundreds of picoseconds) had almost no features of porphyrin transients (Figures 6b and 8b). It had characteristic triplet state spectral features of RuPc at 730 nm. In this case, a simple model of energy transfer from porphyrin to phthalocyanine with a time constant of 26 ps and following fast intersystem crossing, *Ru(CO)Pc^S → *Ru(CO)Pc^T, with a time constant of a few picoseconds was satisfactory. Unlike the dyads, there was relatively a discrepancy between the time constant obtained from transient absorption and emission decay measurements in PhCN, 26 and 11 ps, respectively.

The kinetic parameters of excitation transfer calculated from the up-conversion and pump−probe techniques are listed in Table 1 along with the theoretically estimated values assuming Förster-type energy transfer. It has to be noted that the theoretical estimations were carried out for fixed conformer geometries obtained from the computational modeling. Accounting for the dyad flexibility, the κ^2 values could be overestimated for the ortho dyad and underestimated for the para dyad and pentad. With this in mind, theoretical estimations are in good agreement with the measured rate constant of energy transfer. The results show that the energy transfer rate can be effectively tuned by changing the attachment position of the linker but keeping the overall design of the donor and acceptor units untouched.

The charge transfer was observed only for the dyads in polar solvent, benzonitrile. Unfortunately the time constant for this process cannot be determined from the presented results, since the time limiting step in all cases is the energy transfer, which occurs in the 10−30 ps range depending on the dyad. Further, charge transfer is competing with intersystem crossing, *Ru(CO)Pc^S → *Ru(CO)Pc^T; thus, the time constant for this process has to be 1 ps or less in order to give a detectable

dx.doi.org/10.1021/ic202574q | *Inorg. Chem.* 2012, 51, 3656−3665

population. Alternatively, the charge transfer rate can be obtained by direct excitation of the phthalocyanine chromophore at 655 nm; however, it was not possible with the instrument used. It is also important to note that there was no detectable charge transfer in the pentad. Although this discrepancy is not completely understood, it could be due to some conformational differences in the arrangements of the donor and acceptor in dyad and pentad structures resulting in either a decrease of the rate of the charge transfer or an increase of the rate of intersystem crossing, thus shifting the competition between the two processes in favor of the latter.

The following points emerge from this investigation. (i) There is very good agreement between the theoretically predicted and experimentally determined k_{ENT} values of the dyads with different relative orientations. (ii) The magnitude of k_{ENT} values reveals ultrafast excitation transfer in agreement with the earlier reported H_2P_xIm:MPc (M = Zn or Mg, x = ortho, meta, or para) dyads.[23] (iii) The k_{ENT} values are generally high for the H_2P_oIm:Ru(CO)*Pc* that can be easily ascribed to geometry consideration of the close proximity and favorable orientation of the two macrocycles. (iv) The k_{ENT} value for the H_2P_m(Im:Ru(CO)*Pc*)$_4$ pentad was slightly better than that of the H_2P_pIm:Ru(CO)*Pc* dyad, indicating a higher number of acceptor entities increases the rate of energy transfer in these near-orthogonally positioned donor−acceptor systems. (v) In polar solvent, benzonitrile, the energy transfer in dyads is followed by electron transfer from Ru(CO)*Pc* to H_2P_xIm, which is not observed in nonpolar solvent, toluene, because of the slightly higher energy of the charge-separated state in nonpolar media.

CONCLUSIONS

Using the metal−ligand binding approach, stable molecular dyads and pentad featuring free-base porphyrin and ruthenium carbonyl phthalocyanine were synthesized and spectrally characterized. Unlike previous studies involving ZnPc and MgPc,[23] the current Ru(CO)*Pc* yield stable complexes those could be easily isolated and purified by column chromatography. The molecular structure and electronic states were deduced from computational, spectral, and electrochemical studies. Using steady-state and time-resolved transient absorption techniques, photochemical events taking place in these molecular polyads upon excitation of the free-base entity were systematically investigated. Steady-state emission predicted excitation transfer in which the position of imidazole linkage on the free-base porphyrin entity and the number of Ru(CO)*Pc* entities influenced the efficiency of excitation transfer. The kinetics of energy transfer (k_{ENT}), monitored by performing transient absorption measurements using both upconversion and pump−probe techniques and modeled using the Förster-type energy transfer mechanism, revealed a good match between the theoretically estimated and the experimentally measured kinetic results. The excitation transfer product *Ru(CO)Pc^S instantaneously underwent intersystem crossing to populate *Ru(CO)Pc^T prior to returning to the ground state. Interestingly, the dyads in polar benzonitrile revealed subsequent charge transfer from the excited Ru(CO)*Pc* (product of initial energy transfer) to H_2P, resulting in formation of Ru(CO)$Pc^{+\bullet}$−$H_2P^{-\cdot}$. However, such charge transfer interactions were absent in the case of the pentad in benzonitrile, which could be due to different orientation factors promoting the competing (intersystem crossing) photochemical process.

EXPERIMENTAL SECTION

Chemicals. Free-base 2,11,20,29-tetra-*tert*-butyl-phthalocyanine, *o*-dichlorobenzene, and toluene (in sure seal bottles under nitrogen) were from Aldrich Chemicals (Milwaukee, WI). Tetra-*n*-butylammonium perchlorate, (TBA)ClO_4, was from Fluka Chemicals. All chromatographic materials and solvents were procured from Fisher Scientific and used as received. Syntheses of 5-[1*H*-Imidazol-1-yl)phenyl]-10,15,20-tritolylporphyrin derivatives, H_2P_xIm (x = ortho, meta, or para positions), is given elsewhere.[23]

Synthesis of Carbonyl-2(3),9(10),16(17),23(24)-tetrakis-*tert*-butylphthalocyaninato]Ru(II), Ru(CO)*Pc*.[24] A mixture of tetra-*tert*-butylphthalocyanine (200 mg, 0.26 mmol), $Ru_3(CO)_{12}$ (346 mg, 0.54 mmol), and phenol (13 g) was refluxed at 180−185 °C under argon for 12 h. The reaction mixture was cooled to room temperature, and then it was dissolved 50 mL of ethanol. The resulting solution was dissolved in 200 mL of water and allowed to precipitate. The resulting blue precipitate was filtered, washed with a 4:1 mixture of water and methanol, and dried. The crude was purified by silica gel column chromatography using chloroform as eluent. ^{1}H NMR (400 MHz, $CDCl_3$): 1.90, 1.70, 1.20, (3 s, 36H, $C(CH_3)_3$);), 8.40−7.89, (br m, aromatic 4H), 9.60−8.85, (br m, aromatic 8H). ESI mass in CH_2Cl_2: m/z calcd, 866.03; found, 866.30 (100) $[M]^+$.

5,10,15,20-Tetrakis-4-(1*H*-imidazol-1-yl)phenylporphyrin, H_2P_p(Im)$_4$. To 200 mL of propionic acid, 5.8 mmol (1.0 g) of 4-(1*H*-imidazol-1-yl)benzaldehyde and 5.8 mmol of pyrrole (452 mL) were added. The solution was refluxed for 6 h, and solvent was removed under reduced pressure. The crude was purified on a basic alumina column chromatography with $CHCl_3$:MeOH (92:8 v/v) as eluent. ^{1}H NMR (400 MHz, $CDCl_3$) (in ppm): δ −2.79 (s, 2H), 7.25 (s, 4H, imidazole *H*), 7.58 (s, 4H, imidazole *H*), 7.78 (d, 8H, phenyl *H*), 8.16 (s, 4H, imidazole *H*), 8.28 (d, 8H, phenyl *H*), 8.82 (br s, 8H, β pyrrole). Mass (APCI mode in CH_2Cl_2): calcd, 879.5; found, 880.4

Synthesis of H_2P_xIm:Ru(CO)*Pc* Dyads. A solution of Ru(CO)*Pc* (20 mg, 0.027 mmol) and H_2P_xIm (26 mg, 0.03 mmol) in chloroform (8 mL) was stirred under inert conditions (Ar) at room temperature and protected from light for 18 h. Solvent was evaporated, and the residue was subjected to a silica gel column using hexane:$CHCl_3$ (40:60 v/v) as eluent. **H_2P_oIm:Ru(CO)*Pc*.** ^{1}H NMR (300 MHz, $CDCl_3$): −2.96 (s, 2H), 1.90, 1.73, 1.22, (3 s, 36H, $C(CH_3)_3$) 2.76 (s, 9H), 5.37 (s, 1H, imidazolium H), 6.21 (br s, 2H, imidazole *H*), 6.75−6.83 (m, 4H, phenyl *Hs* next to imidazole moiety) 7.59−9.58 (br m for porphyrin and phthalocyanine aromatic 32H). ESI mass in CH_2Cl_2: m/z calcd, 1588.91; found, 1588.60 (100%) $[M]^+$, 1589.21 (81%). **H_2P_mIm:Ru(CO)*Pc*.** ^{1}H NMR (300 MHz, $CDCl_3$): −2.95 (s, 2H), 1.92, 1.73, 1.22, (3 s, 36H, $C(CH_3)_3$) 2.79 (s, 9H), 5.32 (s, 1H, imidazole H), 5.37 (s, 1H, phenyl H next to imidazole ring), 6.18 (br s, 2H, imidazole *H*), 6.76 (m, 3H, phenyl *Hs* next to imidazole ring) 7.54−9.58 (br m for porphyrin and phthalocyanine aromatic 32H). ESI mass in CH_2Cl_2: m/z calcd, 1588.91; found, 1588.60 (100%) $[M]^+$, 1589.21 (85%). **H_2P_pIm:Ru(CO)*Pc*.** ^{1}H NMR (300 MHz, $CDCl_3$): −2.96 (s, 2H), 1.91, 1.73, 1.21, (3 s, 36H, $C(CH_3)_3$), 2.75 (s, 9H), 5.35 (s, 1H, imidazolium H), 6.18 (br s, 2H, imidazole *H*), 6.80 (dd, 4H, phenyl *Hs* next to imidazole moiety) 7.56−9.58 (br m for porphyrin and phthalocyanine aromatic 32H). ESI mass in CH_2Cl_2: m/z calcd, 1588.91; found, 1588.60 (100%) $[M]^+$, 1589.21 (85%). Yields were in the order of 50−60%,

H_2P_pIm:(Ru(CO)*Pc*)$_4$ Pentad. A solution of Ru(CO)*Pc* (20 mg, 0.027 mmol) and H_2P_p(Im)$_4$ (5.8 mg, 0.03 mmol) in a mixture of chloroform (7 mL) and MeOH (1 mL) was stirred under inert conditions (Ar) at room temperature and protected from light for 24 h. Solvent was evaporated, and the residue was subjected to a silica gel column using hexane:$CHCl_3$ (20:80 v/v) as eluent. ^{1}H NMR (300 MHz, $CDCl_3$): δ −2.79 (s, 2H), 1.25−1.85, (144H, $C(CH_3)_3$) 5.31 (s, 4H, imidazole *H*), 6.05 (br s, 8H, imidazole *H*), 6.91 (dd, 16H, phenyl *H*), 8.01(br s, 8H, β pyrrole *H*), 9.21−9.58 (br multiplet, 48H, *Pc* aromatic *H*). Yield = 45%. ESI mass revealed fragments of dyad, triad, etc., suggesting lower stability of the molecular ion peak under the experimental conditions.

Instrumentation. The optical absorbance measurements were carried out with a Shimadzu model 2550 double-monochromator

dx.doi.org/10.1021/ic202574q | *Inorg. Chem.* 2012, 51, 3656−3665

UV−vis spectrophotometer. The fluorescence emission was monitored using a Varian Eclipse spectrometer. A right angle detection method was used. ^{1}H NMR studies were carried out on Varian 300 MHz and Varian 400 MHz spectrometers. Tetramethylsilane ($Si(CH_3)_4$) was used as an internal standard. Cyclic voltammograms were recorded on a EG&G PARSTAT electrochemical analyzer using a three-electrode system. A platinum button electrode was used as the working electrode. A platinum wire served as the counter electrode, and a Ag/AgCl electrode was used as the reference electrode. Ferrocene/ferrocenium redox couple was used as an internal standard. All solutions were purged prior to electrochemical and spectral measurements using argon gas. Computational calculations were performed by DFT B3LYP/3-21G(*) methods with the GAUSSIAN 03[26] software package on high-speed PCs. Mass spectra were recorded on a Varian 1200 L Quadrupole MS using APCI mode in dry CH_2Cl_2.

Transient Absorption Measurements.[31] An up-conversion instrument (FOG-100, CDP Corp.) for time-resolved fluorescence was used to detect the fast processes with a time resolution of ∼200 fs. The primary Ti:sapphire generator (TiF-50, CDP Corp.) was pumped by a Nd CW laser (Verdi-6, Coherent Inc.), and a second harmonic (∼420 nm) was used to excite the sample solution in a rotating cuvette. Emission from the sample was collected to a nonlinear crystal (NLC), where it was mixed with the so-called gate pulse, which was the laser fundamental. The signal was measured at a sum frequency of the gate pulse and the selected emission maximum of the sample. The gate pulses were passed through a delay line so that it arrived at NLC at a desired time after sample excitation. On scanning through the delay line the emission decay curve of the sample was detected.

Pump−probe and up-conversion techniques for time-resolved absorption and fluorescence, respectively, were used to detect fast processes with a time resolution shorter than 0.2 ps. The instrument and used data analysis procedure have been described earlier.[31]

■ ASSOCIATED CONTENT

Ⓢ Supporting Information

Comparative emission spectra of the investigated compounds with respect to H_2TPP, emission decays, transient absorption component spectra (pump probe) of H_2P_oIm:Ru(CO)*Pc* and H_2P_pIm:Ru(CO)*Pc* dyads in toluene and benzonitrile, and Cartesian coordinates of the optimized geometries of the dyads and pentad. This material is available free of charge via the Internet at http://pubs.acs.org.

■ AUTHOR INFORMATION

Corresponding Author

*E-mail: nikolai.tkachenko@tut.fi (N.V.T.); Francis.DSouza@unt.edu (F.D.).

Notes

The authors declare no competing financial interest.

■ ACKNOWLEDGMENTS

This work was financially supported by the National Science Foundation (grant nos. 1110942 and EPS-0903806) and matching support from the State of Kansas through Kansas Technology Enterprise Corp. and the Academy of Finland. R.J. is thankful to the McNair Scholar Program and the K-INBRI Scholar Program for support.

■ REFERENCES

(1) (a) In *Photosynthetic Protein Complexes; A Structural Approach*; Frome, P., Ed.; Wiley-VCH Verlag GmbH & Co.: Germany, 2008. (b) In *Photosynthetic Light Harvesting*; Cogdell, R., Mullineaux, C., Eds.; Sprigner: Dordrecht, The Netherlands, 2008. (c) In *Handbook of Photosynthesis*, 2nd ed.; Pessarakli, M., Ed.; CRC Press LLC: Boca Raton, FL, 2005. (d) In *Light-Harvsting Antennas in Photosynthesis*; Green, B. R., Parson, W. W., Eds.; Kluwer: Dordrecht, The Netherlands, 2003.

(2) (a) In *The Photosynthetic Reaction Center*; Deisenhofer, J., Norris, J. R., Eds.; Academic Press: San Diego, 1993. (b) Deisenhofer, J.; Epp, O.; Miki, K.; Huber, R.; Michel, H. *J. Mol. Biol.* **1984**, *180*, 385.

(3) (a) In *Photochemical Conversion and Storage of Solar Energy*; Connolly, J. S., Ed.; Academic: New York, 1981. (b) In *Molecular Level Artificial Photosynthetic Materials*; Meyer, G. J., Ed.; Wiley: New York, 1997. (c) Wasielewski, M. R. *Chem. Rev.* **1992**, *92*, 435. (d) Osuka, A.; Mataga, N.; Okada, T. *Pure Appl. Chem.* **1997**, *69*, 797. (e) Flamigni, L.; Barigelletti, F.; Armaroli, N.; Collin, J.-P.; Dixon, I. M.; Sauvage, J.-P.; Williams, J. A. G. *Coord. Chem. Rev.* **1999**, *190−192*, 671. (f) Diederich, F.; Gomez-Lopez, M. *Chem. Rev. Soc.* **1999**, *28*, 263.

(4) (a) Blanco, M.-J.; Consuelo Jimenez, M.; Chambron, J.-C.; Heitz, V.; Linke, M.; Sauvage, J.-P. *Chem. Rev. Soc.* **1999**, *28*, 293. (b) Balzani, V.; Credi, A.; Venturi, M. *ChemSusChem* **2008**, *1*, 26.

(5) (a) Bixon, M.; Fajer, J.; Feher, G.; Freed, J. H.; Gamliel, D.; Hoff, A. J.; Levanon, H.; Möbius, K.; Nechushtai, R.; Norris, J. R.; Scherz, A.; Sessler, J. L.; Stehlik, D. *Isr. J. Chem.* **1992**, *32*, 449. (b) Lewis, F. D.; Letsinger, R. L.; Wasielewski, M. R. *Acc. Chem. Res.* **2001**, *34*, 159.

(6) (a) Gust, D.; Moore, T. A.; Moore, A. L. *Acc. Chem. Res.* **1993**, *26*, 198. (b) Gust, D.; Moore, T. A. In *The Porphyrin Handbook*; Kadish, K. M., Smith, K., Guilard, R., Eds.; Academic Press: San Diego, 2000; Vol. *8*, pp 153−190.

(7) (a) Fukuzumi, S.; Guldi, D. M. In *Electron Transfer in Chemistry*; Balzani, V., Ed.; Wiley-VCH: Weinheim, 2001; Vol. *2*, pp 270−337. (b) Fukuzumi, S. In *The Porphyrin Handbook*; Kadish, K. M., Smith, K., Guilard, R., Eds.; Academic Press: San Diego, 2000; Vol. *8*, pp 115−151. (c) Fukuzumi, S. *Phys. Chem. Chem. Phys.* **2008**, *10*, 2283.

(8) (a) Sakata, Y.; Imahori, H.; Tsue, H.; Higashida, S.; Akiyama, T.; Yoshizawa, E.; Aoki, M.; Yamada, K.; Hagiwara, K.; Taniguchi, S.; Okada, T. *Pure Appl. Chem.* **1997**, *69*, 1951. (b) Imahori, H.; Sakata, Y. *Eur. J. Org. Chem.* **1999**, 2445. (c) Imahori, H.; Tamaki, K.; Araki, Y.; Sekiguchi, Y.; Ito, O.; Sakata, Y.; Fukuzumi, S. *J. Am. Chem. Soc.* **2002**, *124*, 5165. (d) Umeyama, T.; Imahori, H. *Energy Environ. Sci.* **2008**, *1*, 120.

(9) (a) Guldi, D. M. *Chem. Commun.* **2000**, 321. (b) Guldi, D. M. *Chem. Soc. Rev.* **2002**, *31*, 22. (c) Sgobba, V.; Guldi, D. M. *Chem. Soc. Rev.* **2009**, *38*, 165. (d) Mateo-Alonso, A.; Guldi, D. M.; Paolucci, F.; Prato, M. *Angew. Chem., Int. Ed.* **2007**, *46*, 8120. (e) Guldi, D. M. *Phys. Chem. Chem. Phys.* **2007**, *9*, 1400. (f) Sanchez, L.; Nazario, M.; Guldi, D. M. *Angew. Chem., Int. Ed.* **2005**, *44*, 5374.

(10) Sessler, J. S.; Wang, B.; Springs, S. L.; Brown, C. T. In *Comprehensive Supramolecular Chemistry*; Atwood, J. L., Davies, J. E. D., MacNicol, D. D., Vögtle, F., Eds.; Pergamon: New York, 1996; Chapter 9.

(11) (a) El-Khouly, M. E.; Ito, O.; Smith, P. M.; D'Souza., F. *Photochem. Photobiol. C* **2004**, *5*, 79. (b) Chitta, R.; D'Souza, F. *J. Mater. Chem.* **2008**, *18*, 1440. (c) D'Souza, F.; Ito, O. *Chem. Commun.* **2009**, 4913. (d) D'Souza, F.; Ito, O *Chem. Soc. Rev.* **2012**, *41*, 86.

(12) (a) In *Introduction of Molecular Electronics*; Petty, M. C., Bryce, M. R., Bloor, D., Eds.; Oxford University Press: New York, 1995. (b) Molecular Electronics: Science and Technology *Ann. N.Y. Acad. Sci.* **1998**, 852. (c) In *Molecular Switches*; Feringa, B. L., Ed.; Wiley-VCH GmbH: Weinheim, 2001. (d) Gust, D.; Moore, T. A.; Moore, A. L. *Chem. Commun.* **2006**, 1169. (e) Balzani, V.; Credi, A.; Venturi, M. In *Organic Nanostructures*; Atwood, J. L., Steed, J. W., Eds.; 2008, pp 1−31. (f) Tour, J. M. *Molecular Electronics; Commercial Insights, Chemistry, Devices, Architectures and Programming*; World Scientific: River Edge, NJ, 2003.

(13) (a) Imahori, H. *J. Phys. Chem. B* **2004**, *108*, 6130. (b) Li, X.; Sinks, L. E.; Rybtchinski, B.; Wasielewski, M. R. *J. Am. Chem. Soc.* **2004**, *126*, 10810. (c) Giribabu, L.; Kumar, A.; Neeraja, V.; Maiya, B. G. *Angew. Chem., Int. Ed. Engl.* **2001**, *40*, 3621. (d) Aratani, N.; Cho, H. S.; Ahn, T. K.; Cho, S.; Kim, D.; Sumi, H.; Osuka, A. *J. Am. Chem. Soc.* **2003**, *125*, 9668. (e) Shinmori, H.; Ahn, T. K.; Cho, H. S.; Kim, D.; Yoshida, N.; Osuka, A. *Angew. Chem., Int. Ed. Engl.* **2003**, *42*, 2754. (f) Choi, M.-S.; Aida, T.; Yamazaki, T.; Yamazaki, I. *Chem.—Eur. J.* **2002**, *8*, 2667. (g) Choi, M.-S.; Aida, T.; Luo, H.; Araki, Y.; Ito, O.

Angew. Chem., Int. Ed. **2003**, *42*, 4060. (h) Luo, C.; Guldi, D. M.; Imahori, H.; Tamaki, K.; Sakata, Y. *J. Am. Chem. Soc.* **2000**, *122*, 6535. (i) Lazarides, T.; Charalambidis, G.; Vuillamy, A.; Reglier, M.; Klontzas, E.; Froudakis, G.; Kuhri, S.; Guldi, D. M.; Coutsolelos, A. *Inorg. Chem.* **2011**, *50*, 8926.

(14) (a) Seth, J.; Palaniappna, V.; Wagner, R. W.; Johnson, T. E.; Lindsey, J. S.; Holten, D.; Bocian, D. F. *J. Am. Chem. Soc.* **1996**, *118*, 11194. (b) Hsiao, J.-S.; Krueger, B. J.; Wagner, R. W.; Johnson, T. E.; Delaney, J. K.; Mauzerall, D. C.; Fleming, G. R.; Lindsey, J. S.; Bocian, D. F.; Donohoe, R. J. *J. Am. Chem. Soc.* **1996**, *118*, 11181. (c) Seth, J.; Palaniappan, V.; Johnson, T. E.; Prathapan, S.; Lindsey, J. S.; Bocian, D. F. *J. Am. Chem. Soc.* **1994**, *116*, 10578. (d) Bothner-By, A. A.; Dodok, J.; Johnson, T. E.; Delaney, J. K.; Lindsey, J. S. *J. Phys. Chem.* **1996**, *100*, 17551. (e) Wagner, R. W.; Johnson, T. E.; Lindsey, J. S. *J. Am. Chem. Soc.* **1996**, *118*, 11166. (f) Strachan, J. P.; Gentemann, S.; Seth, J.; Kalsback, W. A.; Lindsey, J. S.; Holten, D.; Bocian, D. F. *J. Am. Chem. Soc.* **1997**, *119*, 11191. (g) Li, F.; Gentemann, S.; Kalsbeck, W. A; Seth, J.; Lindsey, J. S.; Holten, D.; Bocian, D. F. *J. Mater. Chem.* **1997**, *7*, 1245. (h) Li, J.; Ambroise, A.; Yang, S. I.; Diers, J. R.; Seth, J.; Wack, C. R.; Bocian, D. F.; Holten, D.; Lindsey, J. S. *J. Am. Chem. Soc.* **1999**, *121*, 8927.

(15) (a) Sessler, J. L.; Magda, D. J.; Harriman, A. *J. Am. Chem. Soc.* **1995**, *117*, 704. (b) Kral, V.; Springs, S. L.; Sessler, J. L. *J. Am. Chem. Soc.* **1995**, *117*, 8881. (c) Springs, S. L.; Gosztola, D.; Wasielewski, M. R.; Kral, V.; Andrievsky, A.; Sessler, J. L. *J. Am. Chem. Soc.* **1999**, *121*, 2281.

(16) (a) D'Souza, F.; Smith, P. M.; Zandler, M. E.; McCarty, A. L.; Itou, M.; Araki, Y.; Ito, O. *J. Am. Chem. Soc.* **2004**, *126*, 7898. (b) D'Souza, F.; Gadde, S.; Islam, D. J. S.; Wijesinghe, C. A.; Schumacher, A. L.; Zandler, M. E.; Araki, Y.; Ito, O. *J. Phys. Chem. A* **2007**, *111*, 8552. (c) Maligaspe, E.; Tkachenko, N. V.; Subbaiyan, N. K.; Chitta, R.; Zandler, M. E.; Lemmetyinen, H.; D'Souza, F. *J. Phys. Chem. A* **2009**, *113*, 8478.

(17) Webber, S. E. *Chem. Rev.* **1990**, *90*, 1469.

(18) Frechet, J. M. *J. Polym. Sci., Part A: Polym. Chem.* **2003**, *41*, 3713.

(19) (a) Takahashi, R.; Kobuke, Y. *J. Am. Chem. Soc.* **2003**, *125*, 2372. (b) Haycock, R. A.; Hunter, C. A.; James, D. A.; Michelsen, U.; Sutton, L. R. *Org. Lett.* **2000**, *2*, 2435. (c) van der Boom, T.; Hayes, R. T.; Zhao, Y.; Bushard, P. J.; Weiss, E. A.; Wasielewski, M. R. *J. Am. Chem. Soc.* **2002**, *124*, 9582. (d) Chen, X.; Drain, C. M. *Encycl. Nanosci. Nanotechnol* **2004**, *9*, 593. (e) Kuramochi, Y.; Satake, A.; Itou, M.; Ogawa, K.; Araki, Y.; Ito, O.; Kobuke, Y. *Chem.—Eur. J.* **2008**, *14*, 2827. (f) Uyar, Z.; Satake, A.; Kobuke, Y.; Hirota, S. *Tetrahedron Lett.* **2008**, *49*, 5484. (g) Kuramochi, Y.; Sandanayaka, A. S. D.; Satake, A.; Araki, Y.; Ogawa, K.; Ito, O.; Kobuke, Y. *Chem.—Eur. J.* **2009**, *15*, 2317.

(20) (a) Smith, K. M. *Porphyrins and Metalloporphyrins*; Elsevier: Amsterdam, 1972. (b) In *The Porphyrin Handbook*; Kadish, K. M., Smith, K. M., Guilard, R., Eds.; Academic Press: San Diego, CA, 2000; Vol. *1*−*20*.

(21) (a) In *Phthalocyanine Materials: Structure, Synthesis and Function*; McKeown, N. B., Ed.; Cambridge University Press: Cambridge, 1998. (b) In *Phthalocyanine: Properties and Applications*; Leznoff, C. C., Lever, A. B. P., Eds.; VCH: New York, 1993. (c) Claessens, C. G.; González-Rodríguez, D.; Torres, T. *Chem. Rev.* **2002**, *102*, 835. (d) Howe, L.; Zhang, J. Z. *J. Phys. Chem. A* **1997**, *101*, 3207−3213. (e) Gunaratne, T. C.; Gusev, A. V.; Peng, X.; Rosa, A.; Ricciardi, G.; Baerends, E. J.; Rizzoli, C.; Kenney, M. E.; Rodgers, M. A. J. *J. Phys. Chem. A* **2005**, *109*, 2078.

(22) (a) Kobayashi, N.; Nishiyama, Y.; Ohya, T.; Sato, M. *J. Chem. Soc., Chem. Commun.* **1987**, 390. (b) Tian, H.-J.; Zhou, Q.-F.; Shen, S.-Y.; Xu, H.-J. *J. Photochem. Photobiol. A* **1993**, *72*, 163. (c) Li, J.; Lindsey, J. S. *J. Org. Chem.* **1999**, *64*, 9101. (d) Yang, S. I.; Li, J.; Cho, H. S.; Kim, D.; Bocian, D. F.; Holten, D.; Lindsey, J. S. *J. Mater. Chem.* **2000**, *10*, 283. (e) Ambroise, A.; Wagner, R. W.; Rao, P. D.; Riggs, J. A.; Hascoat, P.; Diers, J. R.; Seth, J.; Lammi, R. K.; Bocian, D. F.; Holten, D.; Lindsey, J. S. *Chem. Mater.* **2001**, *13*, 1023. (f) Miller, M. A.; Lammi, R. K.; Prathapan, S.; Holten, D.; Lindsey, J. S. *J. Org. Chem.* **2000**, *65*, 6634. (g) Sutton, J. M.; Boyle, R. W. *Chem. Commun.* **2001**, 2014. (h) Kameyama, K.; Satake, A.; Kobuke, Y. *Tetrahedron Lett.* **2004**, *45*, 7617. (i) Zhao, Z.; Nyokong., T.; Maree, M. D. *Dalton Trans.* **2005**, 3732. (j) Tome, J. P. C; Pereira, A. M. V. M; Alonso, C. M. A.; Neves, M. G. P. M. S.; Tome, A. C.; Silva, A. M. S.; Cavaleiro, J. A. S.; Martinez-Diaz, M. V.; Torres, T.; Rahman, G. M. A.; Ramey, J.; Guldi, D. M. *Eur. J. Org. Chem.* **2006**, 257. (k) Ito, F.; Ishibashi, Y.; Khan, S. R.; Miyasaka, H.; Kameyama, K.; Morisue, M.; Satake, A.; Ogawa, K.; Kobuke, Y. *J. Phys. Chem. A* **2006**, *110*, 12734. (l) Giribabu, L.; Kumar, C. V.; Reddy, P. D. *Chem. Asian J.* **2007**, *2*, 1574. (m) Tannert, S.; Ermilov, E. A.; Vogel, J. O.; Choi, M. T. M.; Ng, D. K. P.; Röder, B. *J. Phys. Chem. B* **2007**, *111*, 8053. (n) Soares, A. R. M.; Martinez-Diaz, M. V.; Bruckner, A.; Pereira, A. M. V. M; Tome, J. P. C; Alonso, C. M. A.; Faustino, M. A. F.; Neves, M. G. P. M. S.; Tome, A. C.; Silva, A. M. S.; Cavaleiro, J. A. S.; Torres, T.; Guldi, D. M. *Org. Lett.* **2007**, *9*, 1557. (o) Ali, H.; va Lier, J. E. *Tetrahedron Lett.* **2009**, *50*, 1113. (p) Kojima, T.; Honda, T.; Ohkubo, K.; Shiro, M.; Kusukawa, T.; Fukuda, T.; Kobayashi, N.; Fukuzumi, S. *Angew. Chem., Int. Ed.* **2008**, *47*, 6712.

(23) (a) Maligaspe, E.; Kumpulainen, T.; Lemmetyinen, H.; Tkachenko, N. V.; Subbaiyan, N. K.; Zandler, M. E.; D'Souza, F. *J. Phys. Chem. A* **2010**, *114*, 268. (b) Stranius, K.; Jacobs, R.; Maligaspe, E.; Lemmetyinen, H.; Tkachenko, N. V.; Zandler, M. E.; D'Souza, F. *J. Porphyrins Phthalocyanines* **2010**, *14*, 948.

(24) (a) Rodriguez-Morgade, M. S.; Plonska-Brzezinska, M. E.; Athans, A. J.; Carbonell, E.; de Miguel, G.; Guldi, D. M.; Echegoyen, L.; Torres, T. *J. Am. Chem. Soc.* **2009**, *131*, 10484. (b) Jiménez, A. J.; Grimm, B.; Gunderson, V. L.; Vagnini, M. T.; Calderon, S. K.; Rodríguez-Morgade, M. S.; Wasielewski, M R.; Guldi, D. M.; Torres, T. *Chem.—Eur. J.* **2011**, *17*, 5024.

(25) (a) D'Souza, F.; Ito, O. *Coord. Chem. Rev.* **2005**, *249*, 1410. (b) D'Souza, F.; Ito, O. In *Handbook of Organic Electronics and Photonics*; Nalwa, H. R., Ed.; American Scientific Publishers: New York, 2008; Vol. *1*, Chapter 13, pp 485−521. (c) D'Souza, F.; Ito, O In *Multiporphyrin Array: Fundamentals and Applications*; Kim, D., Ed.; Pan Stanford Publishing: Singapore, 2012; Chapter 8, pp 389−437.

(26) Frisch, M. J.; Trucks, G. W.; Schlegel, H. B.; Scuseria, G. E.; Robb, M. A.; Cheeseman, J. R.; Zakrzewski, V. G.; Montgomery, J. A.; Stratmann, R. E.; Burant, J. C.; Dapprich, S.; Millam, J. M.; Daniels, A. D.; Kudin, K. N.; Strain, M. C.; Farkas, O.; Tomasi, J.; Barone, V.; Cossi, M.; Cammi, R.; Mennucci, B.; Pomelli, C.; Adamo, C.; Clifford, S.; Ochterski, J.; Petersson, G. A.; Ayala, P. Y.; Cui, Q.; Morokuma, K.; Malick, D. K.; Rabuck, A. D.; Raghavachari, K.; Foresman, J. B.; Cioslowski, J.; Ortiz, J. V.; Stefanov, B. B.; Liu, G.; Liashenko, A.; Piskorz, P.; Komaromi, I.; Gomperts, R.; Martin, R. L.; Fox, D. J.; Keith, T.; Al-Laham, M. A.; Peng, C. Y.; Nanayakkara, A.; Gonzalez, C.; Challacombe, M.; Gill, P. M. W.; Johnson, B. G.; Chen, W.; Wong, M. W.; Andres, J. L.; Head-Gordon, M.; Replogle, E. S.; Pople, J. A. *Gaussian 03*; Gaussian, Inc.: Pittsburgh, PA, 2003.

(27) Zandler, M. E.; D'Souza, F. *C. R. Chem.* **2006**, *9*, 960.

(28) (a) Rehm, D.; Weller, A. *Isr. J. Chem.* **1970**, *8*, 259. (b) Mataga, N.; Miyasaka, H. In *Electron Transfer*; Jortner, J., Bixon, M., Eds.; John Wiley & Sons: New York, 1999; Part 2, pp 431−496.

(29) (a) In *Principles of Fluorescence Spectroscopy*, 3rd ed.; Lakowicz, J. R., Ed.; Springer: Singapore, 2006. (b) Förster, T. *Ann. Phys.* **1948**, *437*, 55. (c) Dexter, D. L. *J. Chem. Phys.* **1953**, *21*, 836.

(30) (a) Gouterman, M. *J. Mol. Spectrosc.* **1961**, *6*, 138. (b) Gouterman, M. In *Porphyrins*; Dolphin, D., Ed.; Academic Press: New York, 1978; Vol. 3, Part A, pp 1−165.

(31) (a) Tkachenko, N. V.; Rantala, L.; Tauber, A. Y.; Helaja, J.; Hynninen, P. H.; Lemmetyinen, H. *J. Am. Chem. Soc.* **1999**, *121*, 9378. (b) Vehmanen, V.; Tkachenko, N. V.; Imahori, H.; Fukuzumi, S.; Lemmetyinen, H. *Spectrochim. Acta. A* **2001**, *57*, 2229. (c) Isosomppi, M.; Tkachenko, N. V.; Efimov, A.; Lemmetyinen, H. *J. Phys. Chem. A* **2005**, *109*, 4881.